

Fluctuations of imbalanced fermionic superfluids in two dimensions induce continuous quantum phase transitions and non-Fermi liquid behavior

Philipp Strack

Department of Physics, Harvard University, Cambridge MA 02138, USA

Pawel Jakubczyk

Institute of Theoretical Physics, Faculty of Physics, University of Warsaw, Hoża 69, 00-681 Warsaw, Poland

(Dated: May 6, 2021)

We study the nature of superfluid pairing in imbalanced Fermi mixtures in two spatial dimensions. We present evidence that the combined effect of Fermi surface mismatch and order parameter fluctuations of the superfluid condensate can lead to continuous quantum phase transitions from a normal Fermi mixture to an intermediate Sarma-Liu-Wilczek superfluid with two gapless Fermi surfaces – even when mean-field theory (incorrectly) predicts a first order transition to a phase-separated “Bardeen-Cooper-Schrieffer plus excess fermions” ground state. We propose a mechanism for non-Fermi liquid behavior from repeated scattering processes between the two Fermi surfaces and fluctuating Cooper pairs. Prospects for experimental observation with ultracold atoms are discussed.

I. INTRODUCTION

Understanding the nature of strongly correlated fermion systems, that do not obey the rules of Landau’s Fermi liquid [1, 2], remains one of the most pressing issues in the physics of correlated matter. The unifying property of non-Fermi liquid states are the short lifetimes of quasi-particles. This makes the physics interesting and the theoretical description hard. In strong non-Fermi liquids, there are no well-defined quasiparticles at all, that is, there are no electronic excitations whose lifetime becomes a large timescale when asymptoting energies toward zero. In weak non-Fermi liquids, the interactions of fermions with fluctuations leads to reduced lifetimes and anomalous thermodynamics but ultimately well-defined quasiparticles.

Non-Fermi liquids can occur in a variety of physical contexts: ranging from ceramic copper oxides and transition metal compounds at below-room-temperatures to quantum chromodynamics at finite quark density in conditions similar to those right after the big bang (temperatures of millions of Kelvins) [3–6]. A popular and experimentally relevant scenario for non-Fermi liquid behavior is the proximity to a quantum critical point or phase [7, 8]. The crossover from Fermi liquid to non-Fermi liquid behavior in solid state materials can be induced for example, by changing chemical composition, pressure, or straining the crystal lattice.

Until not so long ago, the best known examples of Fermi liquids accessible in table-top experiments were ^3He [9, 10] and normal metals with low ordering temperatures. Experiments with ultracold atomic quantum gases [11] provide a complementary route to study interacting Fermi systems, sometimes in novel regimes beyond what is possible in solid state situations. Using two-body Feshbach resonances, it is now possible to prepare interacting Fermi gases of (electrically) charge-neutral atoms with tunable interactions in odd-integer, nuclear hyperfine states in the quantum degeneracy regime, that is, at nano-Kelvin temperatures corresponding to fractions of the Fermi temperature [12–14].

Density- and/or mass-imbalanced Fermi mixtures [15–17]

represent such a new beyond-solid-state synthetic quantum material. A bold proposition by Liu and Wilczek [18] on pairing in such fermion mixtures invoked a homogeneous superfluid coexistent with “metallic” fermions on two Fermi surfaces triggered research on Sarma’s earlier proposal [19] as well as various generalization into the modern context of ultracold Fermi gases [20–30].

The common point of departure for these analysis is the attractively interacting (spin-) polarized Fermi gas

$$H = \sum_{\mathbf{k}\sigma} \xi_{\mathbf{k}\sigma} c_{\mathbf{k}\sigma}^\dagger c_{\mathbf{k}\sigma} + \frac{g}{V} \sum_{\mathbf{k}, \mathbf{k}', \mathbf{q}} c_{\mathbf{k}+\mathbf{q}/2, \uparrow}^\dagger c_{-\mathbf{k}+\mathbf{q}/2, \downarrow}^\dagger c_{\mathbf{k}'+\mathbf{q}/2, \downarrow} c_{-\mathbf{k}'+\mathbf{q}/2, \uparrow}, \quad (1)$$

where the dispersion of the two spin-components is $\xi_{\mathbf{k}\sigma} = \frac{\mathbf{k}^2}{2m_\sigma} - \mu_\sigma$ with $\sigma = \uparrow, \downarrow$, and $g < 0$ is an attractive, structureless contact interaction between the species. Each dispersion is inflection symmetric $\xi_{\mathbf{k}\sigma} = \xi_{-\mathbf{k}\sigma}$. V is the volume and in general the masses m_σ and chemical potentials μ_σ of each spin species can be different.

A mean-field diagonalization of Eq. (1) around the static and homogeneous projection of superfluid fermion bilinear containing one fermion from each spin species, $\alpha = \lim_{q \rightarrow 0} \int_k \psi_{k+\frac{q}{2}\uparrow} \psi_{-k+\frac{q}{2}\downarrow}$, produces two quasi-particle branches in the superfluid phase

$$E_\pm = \frac{\xi_{\mathbf{k}\uparrow} - \xi_{-\mathbf{k}\downarrow}}{2} \pm \sqrt{\frac{\alpha^2}{2} + \left(\frac{\xi_{-\mathbf{k}\downarrow} + \xi_{\mathbf{k}\uparrow}}{2}\right)^2}, \quad (2)$$

where the condition $\xi_{\mathbf{k}\sigma} = 0$ defines the (bare) Fermi surfaces of the two species in the normal phase. This quasi-particle energies can have zeros at finite α , as shown in Fig. 1, such that the superfluid state can have Fermi surfaces for certain parameters.

Such an exotic superfluid would be an intriguing state of matter: translated to the correlated electron context, it would be a ‘perfect metal’ with large Fermi surfaces and a superconductor at the same time. This is in stark contrast to both, conventional (s-wave) BCS-superconductors and high-temperature superconductors: in conventional superconductors, the superfluid order parameter gaps out the entire Fermi

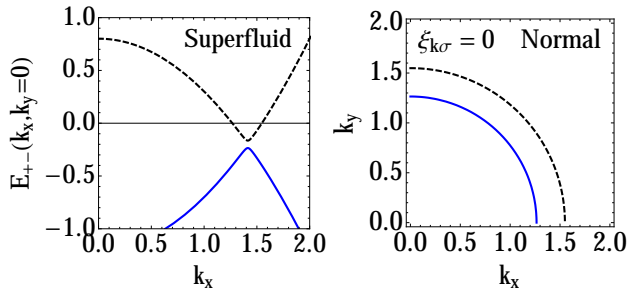


FIG. 1: (Color online) Superfluid: Meanfield quasi-particle energies in the superfluid phase (left). Normal: Mismatched Fermi surfaces in the normal phase (right). The smaller, blue Fermi surface is taken to be the \downarrow -component, the larger, black-dashed Fermi surface belongs to the \uparrow -component. Here and in the rest of the paper we use $\mu = \frac{\mu_{\uparrow} + \mu_{\downarrow}}{2}$ as the average chemical potential and $h = \frac{\mu_{\uparrow} - \mu_{\downarrow}}{2}$ as the average “Zeeman” field. We further define the mass ratio as $r = \frac{m_{\downarrow}}{m_{\uparrow}}$. The Fermi momenta of the two species are given by $k_{F,\uparrow} = \sqrt{2(\mu + h)}$ and $k_{F,\downarrow} = \sqrt{2r(\mu - h)}$. Here we used $r = 1$ in units of m_{\uparrow} as appropriate for a equal-mass mixtures, $\mu = 1$, $h = 0.1$, and $\alpha = 0.05$. The superfluid “gap” α opens away from the Fermi surfaces [18, 19] (where the black-dashed line E_+ crosses zero).

surface and charge transport occurs exclusively via bosonic Cooper pairs; in the high-temperature superconductors, the gap has a d-wave structure leaving nodes on the Fermi surface unpaired, however with energetically suppressed density of states.

In the Sarma-Liu-Wilczek superfluid, the simultaneous presence of strong phase fluctuations, that is, the Goldstone mode and the gapless fermions makes this a strongly correlated “soup” with anomalous transport thermodynamic properties that are not fully understood. Endowing such a state with momentum structure in the gap or lattice potentials would complement efforts on high-temperature superconductors where exotic states of matter with (sometime fractionalized) Fermi surfaces are coupled to gapless degrees of freedoms such as gauge bosons.

Parish *et al.* [24] presented a comprehensive mean-field picture of the imbalanced Fermi gas problem at finite temperatures (focusing on the case of dimensionality $d = 3$). In particular, they emphasized the possibility of suppressing the temperature of the tricritical point [31] by increasing the mass-imbalance between the two fermion species. However, it is rather clear that the picture of Refs. 24, 31 is not fully realistic in two spatial dimensions, $d = 2$. The first- (or second-) order transition to the superfluid state at $T > 0$ implies the existence of long-ranged order and therefore contradicts the Mermin-Wagner theorem. The important role of fluctuations is also clearly signaled in the recent study [32], operating at Gaussian level. A complete theory accounting for fluctuations should instead (most likely) yield a Berezinski-Kosterlitz-Thouless (BKT) type superfluid involving no true long-ranged order. It is on the other hand well known that the BKT transition is actually of infinite order, so that the free energy is of the C^∞ class, but not an analytic function. The occurrence of a tricritical point in the phase diagram is therefore not admissible,

	Broken symmetry	Collective momentum	Effective model	Bare collective dynamics
Spin-density wave	SU(2) spin rotation	Commensurate $Q=(\pi, \pi)$ particle-hole pair (Ferromagnet at $Q=(0,0)$ also possible)	Hot spots on Fermi surface coupled to magnon	$ \Omega $, $z = 2$ 2 Goldstone modes
Nematic Fermi surface deformation	C_4 lattice orientation	Forward scattered $Q=(0,0)$ particle-hole pair	One Fermi surface coupled to photon	$ \Omega / q $, $z = 3$ No Goldstone mode
Imbalanced superfluids	U(1) number conservation	Homogeneous $Q=(0,0)$ particle-particle pair (LOFF at finite Q also possible)	Two mismatched Fermi surfaces coupled to Cooperon	$i\Omega$, $z = 2$ 1 Goldstone mode

■ : proposed in this paper

FIG. 2: (Color online) Plain-vanilla non-Fermi liquid “metal” quantum phase transitions at finite fermion density in two spatial dimensions. This plain-vanilla classification excludes exotic scenarios such as e.g.: topological order, fractionalization/emergent gauge field or transitions to fully insulating states. Non-Fermi liquid properties of the spin-density wave and Fermi surface deformation cases have recently been discussed for example in Ref. 47–52. The interplay with spatially inhomogenous Larkin-Ovchinnikov-Fulde-Ferrell (LOFF) states is discussed in the text.

except at $T = 0$.

The bottom line of the previous work was that, in the relatively weakly interacting BCS regime of Eq. (1), mismatching the Fermi surfaces typically lead to abrupt, first-order Clogston transitions [33] out of the superfluid state into a phase-separated (in real space) state, containing superfluid and normal puddles, which possessed the lowest energy among several candidate states [20–22, 24, 26]. However, most of these analysis have relied on mean-field theory or focussed on three dimensional Fermi mixtures.

It is worthwhile noting that fluctuation effects are known to change the basic properties of phase transitions in a number of important systems, in low dimensionalities in particular. It seems that more commonly fluctuations favor the first-order scenario. For a review on the classical systems we refer to [34]. On the quantum side, we mention the fluctuation-induced first-order quantum phase transitions in itinerant magnets and superconductors [35, 36] and the quantum variant of the Imry-Ma phenomenon recently established rigorously [37]. This was also firmly recognised that a wide class of metallic phase transitions is first order at low temperatures, but (by necessity) second-order at sufficiently high T [38].

II. KEY RESULTS

This paper addresses the impact of order parameter fluctuations on imbalanced superfluids in interacting Fermi mixtures in two dimensions. We propose here the possibility of a new type of fluctuation-induced quantum criticality between imbalanced superfluids and a normal Fermi gas as realizable with present-day experimental technology in the relatively weakly interacting BCS regime. We have written this paper hoping that the fluctuation-induced quantum criticality of superfluid, charge-neutral Fermi mixtures will become a fruitful addition

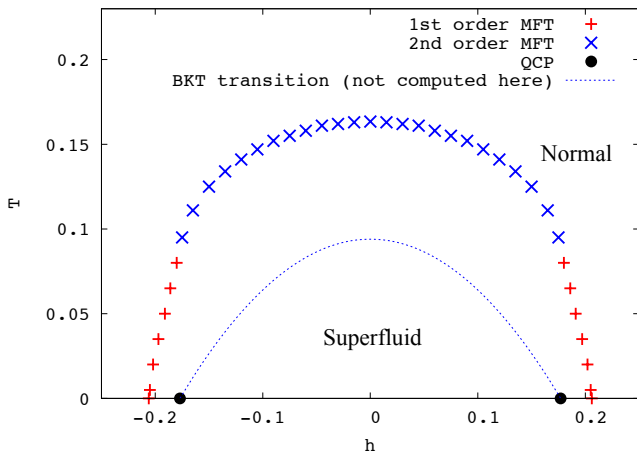


FIG. 3: (Color online) Fluctuation-corrected phase diagram of imbalanced fermionic superfluids in two dimensions. Goldstone and longitudinal fluctuations induce new quantum critical points (black circles) at $(h = \pm 0.18, T = 0)$ between a normal Fermi mixture and a Sarma-Liu-Wilczek superfluid with gapless fermions. Toward $h \rightarrow 0$, another transition to a fully gapped superfluid is expected. Furthermore fluctuations suppress spontaneous symmetry breaking to $T = 0$. Extension of our computations to finite T [69] would lead to a BKT transition line connecting the new QCPs [70]. Mean-field theory (MFT) predicts an incomplete picture: a superfluid dome (blue crosses) with long-range order and 1st order transitions on its wings (red crosses).

to the “plain vanilla” set of non-Fermi liquid quantum critical points at finite fermion density tabulated in Fig. 2. To substantiate this claim, we here pursue two complementary directions:

In Sec. III, we present first computational evidence that strong phase and amplitude fluctuations of the superfluid order parameter suppress the regime of phase-separation and lead to a continuous quantum phase transition between an imbalanced Sarma-Liu-Wilczek superfluid with gapless Fermi surfaces and a normal mixture as shown in Fig. 3. This phase diagram is based on the solution of a partial differential (renormalization group flow) equation for the effective potential/free energy density of the Fermi mixture $U(\alpha)$. The possibility of a quantum phase transition from a state of “2 Fermi surfaces + BEC” to “2 Fermi surfaces and no BEC” was alluded to in the different microscopic context of mixtures of fermions with fundamental bosons [53]. Because of the fundamental nature of the boson in Ref. 53, this transition does not fall into the plain-vanilla non-Fermi liquid “metal” categorization of Fig. 2, which restricts to purely fermionic systems.

In Sec. IV, we analyze the diagrammatics of the effective field theory coupling the collective “Cooperon” to two mismatched Fermi surfaces. Non-Fermi liquid physics appears at two-loop order, despite the fact that the Cooperon reconstructs the fermion dispersions away from the Fermi surfaces. Behind this are repeated scattering processes involving Cooperons and off-shell particle-hole pairs of the respective *other* species as shown in Fig. 4. This enhances the scattering rate

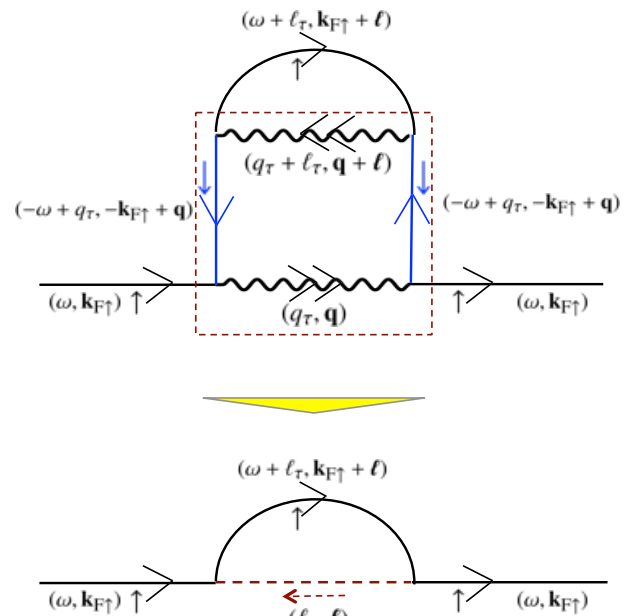


FIG. 4: (Color online) Repeated scattering of Cooperons and particle-hole pairs of cold, off-shell fermions (red, dashed box in upper graph) mediates a singular, intra-species interaction (red, dashed line in bottom graph) that induces non-Fermi liquid behavior on the Fermi surfaces. Wiggly line here denotes the one-loop dressed (cf. Fig. 9) Cooper pair propagator.

around the Fermi surface which should be observable with experimental techniques such as rf-spectroscopy [17, 39]. One may therefore say, on mean-field level, both Fermi surfaces remain “cold” at the superfluid transition. Beyond mean-field, however, order parameter fluctuations “warm them up” leading to faster than Fermi liquid decay rates but probably ultimately stable quasi-particles. Different, interesting mechanisms to achieve non-Fermi liquid features with imbalanced Fermi gases were given in Refs. 41, 46. Putting the attractively interacting Fermi mixture into spin-dependent optical lattices [27], that deform the bare Fermi surfaces such that “band-crossing” are generated, also naturally leads to non-Fermi liquid physics from pairing at least close to the “hot” crossing points.

Our results of Secs. III, IV undoubtedly point out the qualitative importance of fluctuations to the physics of imbalanced superfluids in two dimensions. Like any other quantum critical point for interacting Fermi systems at finite density, however, fluctuations in the vicinity of the QCPs (black dots in Fig. 3) will attract competition from other instabilities. To this end, two important aspects should be investigated further.

The first one is the interplay with induced intra-species p-wave superfluidity [23, 56], whose ordering scales, however, are expected to be very small in the relatively weakly interacting BCS regime. In fact, there are similarities to the case of induced *d-wave pairing* close to antiferromagnetic critical points in metals [47, 54]. There, singular magnetic fluctuations have two counter-acting effects: they reduce the amount of electronic spectral weight around the Fermi surfaces (especially the hot spots), and at the same time they generate loga-

rithmic singularities in the d-wave pairing channel. A similar competition occurs here in imbalanced superfluids: singular Cooper pair fluctuations generate intra-species pairing tendencies in the p-wave channel; at the same time the lifetimes of quasiparticles around the Fermi surfaces are reduced by the mechanism of Fig. 4.

The second open question is the interplay with translational symmetry breaking tendencies from inhomogeneous LOFF pairing (see for example [40, 41, 44, 45] for analysis in one-dimensional systems). As pointed out by Lamacraft [41], scattering off singular Cooperons with spatial modulation is a natural route to non-Fermi liquid behavior because it directly connects the mismatched Fermi surfaces. At the mean-field level, Sheehy and Radzihovsky provided a comprehensive analysis of the imbalanced Fermi gas in the continuum [42] with the result that the inhomogeneous LOFF states occupies only a very narrow strip in the phase diagram. A very recent study [32] emphasises the prominent role of fluctuations in $d = 2$ and suggests that (even at the Gaussian level) the LOFF states are unstable at $T > 0$.

In lower dimensionality $d < 2$ and under inclusion of lattice potentials, periodic modulations of the phase and or the amplitude of the superfluid order parameter can be stabilized at the mean-field level [43] and an extension of our theory to this case is an interesting future direction. A fluctuation theory beyond Gaussian level for this case is significantly more complicated: in addition to the global (number) charge symmetry, also continuous translation symmetry is broken leading to an additional Goldstone ‘‘phonon’’ in the fluctuation spectrum. One would then deal with a non-Fermi liquid coupled to a damped, bosonic sector of the $O(4)$ universality class.

We conclude in Sec. V and give a brief outlook on experimental observation with ultracold quantum gases.

III. FUNCTIONAL FLOW TO CRITICALITY

For interacting Fermi systems at the brink of phase-separating and abrupt jumps of the order parameter (as is the case in the mean-field theory for imbalanced Fermi mixtures at low temperatures), an expansion of the effective potential in powers of the order parameter is not possible. The approach Ref. [55] proposed to integrate a *functional* flow equation of the local potential along a continuous flow parameter Λ this way capturing order parameter fluctuations keeping the *entire* local potential on a discrete set of points in field space. The initial conditions for this flow at the scale Λ_0 (the characteristic energy below which collective order parameter fluctuations become important) is given by the mean-field effective potential of Eq. (1)

$$U^{\Lambda=\Lambda_0}(\alpha) = \frac{-1}{2g}\alpha^2 - T \sum_{k_0, \mathbf{k}} \ln \left[\frac{(-ik_0 + \xi_{\mathbf{k}\uparrow})(ik_0 + \xi_{-\mathbf{k}\downarrow}) + \alpha^2/2}{(-ik_0 + \xi_{\mathbf{k}\uparrow})(ik_0 + \xi_{-\mathbf{k}\downarrow})} \right], \quad (3)$$

where α is the real-valued ordering field (the longitudinal σ -direction in the local, Mexican hat potential that involves all powers of the ordering field). The mean-field theory is derived



FIG. 5: (Color online) Graphical representation of the flow equation Eq. (4) involving traces over field (α -dependent Goldstone (wiggly loop) and longitudinal (dashed loop) propagators, respectively. Grey dots denote cutoff insertions.

in Appendix A. The transverse Goldstone quantum field will be denoted by π . In two dimensions, the attractive interaction $g(\Lambda_{\mathbf{k}_F}) = -\frac{2\pi}{m \ln[a_{2D}\Lambda_{\mathbf{k}_F}]}$ changes logarithmically with momentum scale [57, 58] and we will evaluate it at a characteristic scale of the order of the Fermi momenta involved, $\Lambda_{\mathbf{k}_F}$. The particle-particle ladder for two particles in vacuum has a logarithmic singularity for small and large momenta. Therefore, two particles form a bound state for arbitrarily weak attraction among them [59, 60]. Here a_{2D} is the 2D scattering length. This paper restricts to the BCS regime, $|\Lambda_{\mathbf{k}_F}|a_{2D} \gg 1$ such that gaps are relatively small and we are well separated from the strong-coupling region where the crossover to the BEC regime sets in [58]. We may therefore expect BCS-BEC crossover-like contractions of the Fermi volumes [61] to be subdominant and we perform our calculations at constant chemical potentials (using their difference as the tuning parameter).

We now proceed to integrate order parameter fluctuations with the functional flow equation for the effective potential

$$\partial_\Lambda U^\Lambda(\alpha) = \frac{1}{2} \text{tr}_q \left[\partial_\Lambda R^\Lambda(q) \left(G_{\sigma\sigma}^R(q; \alpha) + G_{\pi\pi}^R(q; \alpha) \right) \right]. \quad (4)$$

where $\text{tr}_q = T \sum_{q_\tau} \int \frac{d^2\mathbf{q}}{(2\pi)^2}$ stands for frequency and momentum integrations over the field-dependent Goldstone and longitudinal loops shown in Fig. 5. At vanishing cutoff scale $\Lambda \rightarrow 0$ all the fluctuation modes are incorporated into the partition function and $F(\alpha) = \lim_{\Lambda \rightarrow 0} U^\Lambda(\alpha)$ is the free energy density. Both, the longitudinal propagator $G_{\sigma\sigma}^R(k; \alpha)$ and the Goldstone propagator $G_{\pi\pi}^R(k; \alpha)$ are explicitly field (α)-dependent

$$G_{\pi\pi}^R(q; \alpha) = \frac{Z_\Omega(\alpha_0)q_\tau^2 + Z_q(\alpha_0)\mathbf{q}^2 + m_{\pi R}^2(\alpha, R)}{\det^R(q; \alpha)} \quad (5)$$

$$G_{\sigma\sigma}^R(q; \alpha) = \frac{Z_\Omega(\alpha_0)q_\tau^2 + Z_q(\alpha_0)\mathbf{q}^2 + m_{\sigma\sigma}^2(\alpha, R)}{\det^R(q; \alpha)}.$$

The above expressions involve an approximation, treating the Z -factors as constants (see below). The ‘‘mass’’ terms for the Goldstone boson $m_{\pi R}^2(\alpha) = U'(\alpha) + R^\Lambda(q)$ and the longitudinal propagator $m_{\sigma R}^2(\alpha) = U'(\alpha) + \alpha^2 U''(\alpha) + R^\Lambda(q)$ involve a regulator $R^\Lambda(q)$, to be specified below, and are evaluated at general α . Here, $U'(\alpha)$ is a first, and $U''(\alpha)$ is the second field derivative with respect to $\rho = \frac{1}{2}\alpha^2$. The determinant in (σ, π) field space is

$$\det^R(q; \alpha) = \left(Z_\Omega(\alpha_0)q_\tau^2 + Z_q(\alpha_0)\mathbf{q}^2 + m_{\sigma\sigma}^2(\alpha, R) \right) \times \left(Z_\Omega(\alpha_0)q_\tau^2 + Z_q(\alpha_0)\mathbf{q}^2 + m_{\pi\pi}^2(\alpha, R) \right) + X^2(\alpha_0)q_\tau^2. \quad (6)$$

The Z - and X -factors are frequency and momentum renormalization factors and are evaluated at the minimum of the effective potential α_0 . In the superfluid phase away from the critical point, σ and π components of the Z -factors can exhibit very different scaling properties in the infrared [62, 63]. Since our main interest here is the phase diagram and not the infrared asymptotics, we will keep here only one set of Z - and X -factors. The X -factor multiplies a linear time-derivative $G_{\sigma\pi}^R \sim Xq_\tau$ and couples the Goldstone and longitudinal fluctuations. In the present renormalization scheme we supplement only the diagonal components of the inverse propagator with the cutoff term R . Within such a procedure, there arises no contribution from $G_{\sigma\pi}^R$ in Eq. (4) and the impact of the X -factor on the flow of U occurs only via the determinant.

Eq. (4) emerges upon evaluating the exact flow equation for the generator of 1-particle-irreducible vertices [64] at a uniform field configuration. The resultant formula involves field- and scale- dependent Z and X factors. The essence of the approximation leading to the closed set Eq. (4-6) amounts to disregarding these dependencies. An important ingredient of the present study resides in the local potential Eq. (3), which is the starting point of for the solution of Eq. (4), and which is directly and clearly related to the microscopic, fermionic system (see Appendix A for a derivation).

Let us also note that Eq. (4-6) fulfill the Mermin-Wagner theorem [65] upon turning on a temperature, and provide a framework to study quantum fluctuations beyond BCS-theory in a superfluid state *without* violating Goldstone's theorem, that is, without generating an unphysical Goldstone mass [63, 66, 67]. This is because the flow of the minimum of the potential α_0 is self-consistently determined from the condition (Ward identity) that the (unregulated) Goldstone mass $m_{\pi,R=0}[\alpha_0]^2 = U'[\alpha] \equiv 0$ vanishes for all Λ .

We now present our results from solving the functional flow of Eq. (4-6). Using a combined frequency and momentum cutoff $R_\Lambda(q_\tau, \mathbf{q}) = Z_q(\Lambda^2 - q^2 - \frac{Z_\Omega}{Z_q} q_\tau^2)\theta(\Lambda^2 - q^2 - \frac{Z_\Omega}{Z_q} q_\tau^2)$ the frequency and momentum integrations can be performed and Eq. (4) becomes

$$\Lambda \partial_\Lambda U_\Lambda(\rho) = -\frac{\tilde{Z}\Lambda^2}{4\pi^2} (M_{\sigma\sigma}(\rho) + M_{\pi\pi}(\rho)) \times \left\{ -\frac{\tilde{Z}\Lambda}{X^2} + \left(\frac{\Lambda^2}{X\sqrt{M_{\pi\pi}(\rho)M_{\sigma\sigma}(\rho)}} + \frac{\tilde{Z}^2\sqrt{M_{\pi\pi}(\rho)M_{\sigma\sigma}(\rho)}}{X^3} \right) \arctan \left[\frac{\Lambda X}{\tilde{Z}\sqrt{M_{\pi\pi}(\rho)M_{\sigma\sigma}(\rho)}} \right] \right\}. \quad (7)$$

with $\rho = \alpha^2/2$, $\tilde{Z} \equiv \sqrt{\frac{Z_\Omega}{Z_q}}$, the regulated longitudinal mass $M_{\sigma\sigma}(\rho) \equiv Z_q\Lambda^2 + U'(\rho) + 2\rho U''(\rho)$ and the regulated Goldstone mass $M_{\pi\pi}(\rho) \equiv Z_q\Lambda^2 + U'(\rho)$.

Eq. (7) is a second-order partial differential equation, which we solve numerically on a grid in field space containing up to 200 points, where the non-zero minimum (initial) is situated around the middle of the box. The initial condition for $U(\alpha)$ is the un-truncated, mean-field effective potential containing all orders in the order parameter field.

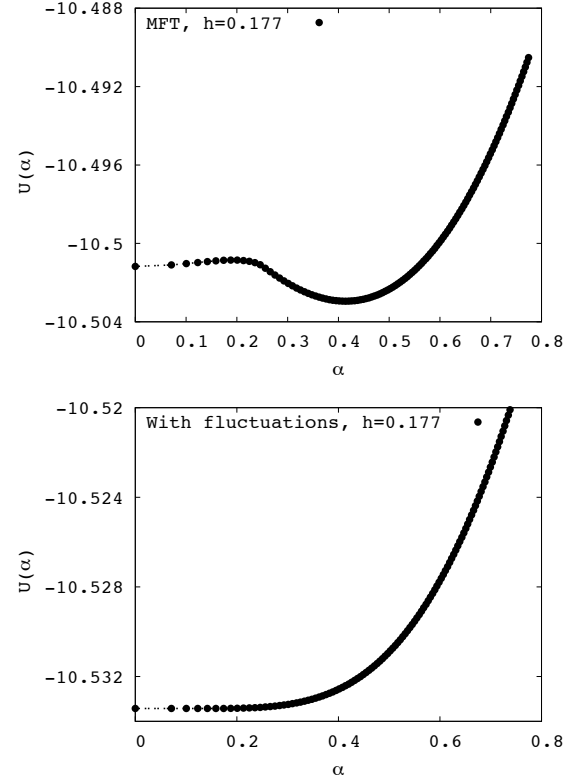


FIG. 6: (Color online) Comparison of the zero-temperature potentials at the new QCP (black circles at $h = 0.177$, $T=0$ in Fig. 3). Mean-field theory (top) incorrectly predicts a phase-separated fully gapped BCS + excess fermion state with the global minimum at $\alpha_0 = 0.42$, which overshadows the Fermi surface mismatch. Fluctuations (bottom) smear out the curved region in the potential, and in fact lead to a quantum phase transition with continuously onsetting superfluid order α_0 slightly above zero. Numerical parameters and initial values of the Z - and X -factors are: $g = -2$, $Z_\Omega^{\Lambda_0} = Z_q^{\Lambda_0} = 1$, and $X^{\Lambda_0} = 0.2$. Further technical details are given in Appendix B.

As described in Fig. 3, fluctuations may have a drastic effect on the even qualitative features of the phase diagram. Here, quantum fluctuations suppress the first-order transition and associated phase separation between a BCS + excess fermion state and instead indicate a continuous quantum phase transition to a superfluid state with two Fermi surfaces, which could exist as an intermediate phase. Upon further increasing the interaction or reducing the imbalance h , this is expected to become a fully gapped BCS state with no Fermi surface transiting over a state one Fermi surface with enhanced density of states (when the black-dashed quasi-particle branch in Fig. 1 is pushed upwards by larger values of the gap $\alpha > h$) [22]. Note that the most significant renormalization of the potential $U(\rho)$ occurs relatively early in the flow (intermediate Λ), where the key effect is that regions with large curvature are smoothed out by quantum fluctuations. Figs. 6 and 7 exhibit a comparison of the mean-field potential with its renormalized version at various points in the phase diagram.

Let us observe that the above situation does not occur for sufficiently large absolute values of the coupling g , in which

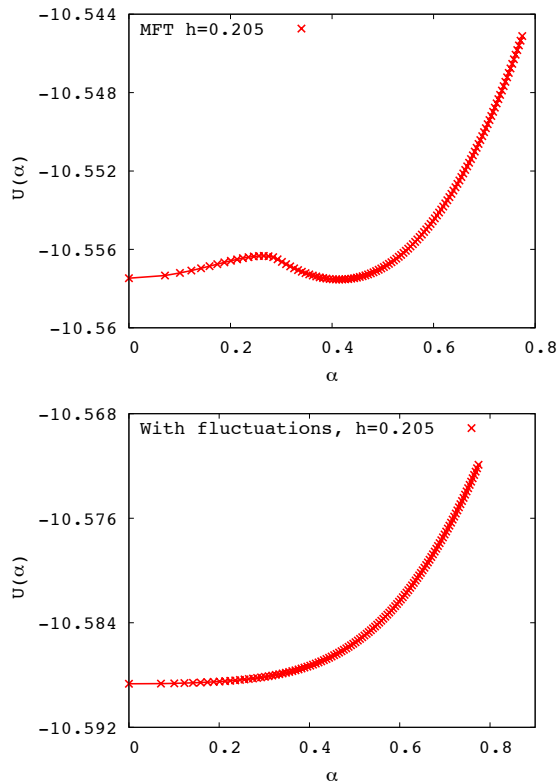


FIG. 7: (Color online) Comparison of the zero-temperature potentials at the putative mean-field first order transition (red cross at $h = 0.205$, $T = 0$ in Fig. 3). Mean-field theory (top) incorrectly predicts a first-order transition to a phase-separated fully gapped BCS + excess fermion state with a second minimum at $\alpha_0 = 0.41$ degenerate to the $\alpha_0 = 0$ one, the former overshadowing the Fermi surface mismatch. Fluctuations (bottom), however, suppress the ordering tendencies and instead yield a symmetric state with $\alpha_0 = 0$. The other initial parameters are the same as in Fig. 6.

case fluctuations are not sufficiently potent to induce a QCP and the transition at $T = 0$ remains first-order also after renormalization. By tuning g one goes between the two possibilities crossing the specific value of g , where the system displays a quantum tricritical point.

We also note here the reassuring feature of Eqs. (4,7) that at any finite T , a solution with a finite minimum α_0 , which would indicate spontaneous symmetry-breaking is not permissible. This is because of a logarithmic running of α_0 from the Goldstone loop such that $\alpha_0 \rightarrow 0$ for $\Lambda \rightarrow 0$ at finite T .

We close this section by noting that the ultimate fate of the intermediate gapless superfluid in two dimensions will also depend strongly on fermionic self-energy effects, such as those discussed in the next Sec. IV and fluctuations in the shape of the Fermi surfaces, and the interplay with competing instabilities. An intriguing scenario [71] is the possibility of a merging of the two QCP's in Fig. 3 to form an isolated QCP at $(h = 0, T = 0)$ indicating the absence of any superfluid phase in the ground state. Resolution of such possibilities requires studying the interplay of the bosonic potential and single-particle, fermionic effects.

IV. NON-FERMI LIQUID MECHANISM

We now outline how the single-fermion properties are affected by order parameter fluctuations at the imbalanced superfluid quantum phase transition. To this end, we first write down the effective quantum field theory coupling the two mismatched Fermi surfaces to the (bosonic) Cooper pairing field containing one fermion from each Fermi surface. We then present a repeated scattering mechanism that is expected to reduce the lifetime of the quasiparticles around the Fermi surfaces leading to deviations from the Fermi liquid.

The relevant Lagrangian density contains the propagators of the two Fermion species

$$\mathcal{L}_{\bar{\psi}\psi} = \bar{\psi}_{k\uparrow}(-ik_\tau + \xi_{k\uparrow})\psi_{k\uparrow} + \bar{\psi}_{k\downarrow}(-ik_\tau + \xi_{k\downarrow})\psi_{k\downarrow}, \quad (8)$$

with $\xi_{k\sigma}$ fermion dispersions leading to two mismatched Fermi surfaces (Fig. 8), a complex-valued, dynamical Cooper pairing field

$$\mathcal{L}_{\phi^*\phi} = \phi_q^* \left(-X iq_\tau + Z_\Omega q_\tau^2 + Z_q \mathbf{q}^2 + r \right) \phi_q, \quad (9)$$

whose leading frequency (q_τ) and momentum (\mathbf{q}) dependence is determined by the particle-particle bubble explained in Fig. 9. r is the usual control parameter; we will here be focussed on the quantum critical point where $r = 0$. The complex, linear frequency term determines the bare collective dynamics to have dynamical exponent $z = 2$. Note that the Cooperon propagator Eq. (9) is only valid when frequencies q_τ and momenta \mathbf{q} are small when compared to the Fermi energy. At higher scales, the bi-fermion character of the ϕ bosons results in a (decay) continuum and branch cuts in the complex plane, as per the logarithm of Eq. (C4); then the simple pole structure of Eq. (9) is insufficient to describe the collective dynamics properly. Expanding this logarithm gives the expressions for the X - and Z -factors (see Appendix C).

The Cooper pairs are coupled to the pair of mismatched Fermi surfaces via a Yukawa coupling with strength g

$$\mathcal{L}_{\psi\phi} = g \left(\phi_q \bar{\psi}_{-k+\frac{q}{2}\uparrow} \bar{\psi}_{k+\frac{q}{2}\downarrow} + \phi_q^* \psi_{k+\frac{q}{2}\downarrow} \psi_{-k+\frac{q}{2}\uparrow} \right) \quad (10)$$

such that they can decay and recombine into fermions. Ref. 53 wrote down related critical field theories for Bose-Fermi mixtures with the aim of describing Fermi-Bose molecule formation of the fermions with fundamental bosons.

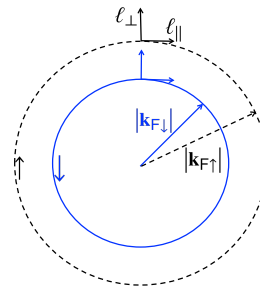


FIG. 8: (Color online) Mismatched Fermi surfaces and local coordinate systems in momentum space.

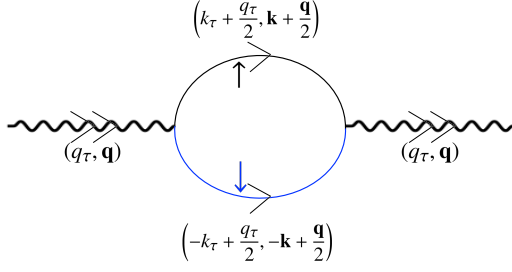


FIG. 9: (Color online) Imbalanced particle-particle bubble that determines the collective Cooper pair dynamics (the X and Z -factors) given in Eq. (9). Generalized to the superfluid phase, fermionic contractions of this form determine the initial values of the Goldstone and longitudinal propagators in the renormalization group flow of Eqs. (5,6). Wiggly line is the bosonic Cooper pair propagator, blue straight line the spin-down fermion propagators and, black straight line the spin-up fermion propagator. The cubic vertex connecting the three is the Yukawa coupling.

We now analyze the structure of the repeated scattering mechanism off finite (q_τ, \mathbf{q}) fluctuations at the quantum critical point. The single-scattering event of Fig. 10 is infrared finite because the respective, internal fermion line is always evaluated off-shell, that is, away from its Fermi surface. Replacing the blue (spin-down) fermion line with a constant, the phase measure from the q_τ and \mathbf{q} integration yields an (infrared) finite integral over the massless Cooper pair propagator with $z = 2$ dynamics. The leading infrared-dangerous scattering process for the frequency-dependent self-energy of the spin-up Fermi surfaces, $\Sigma_\uparrow(\omega, \mathbf{k}_{F\uparrow})$, is a two-loop contraction shown in the top of Fig. 4:

$$\begin{aligned} \Sigma_\uparrow(\omega, \mathbf{k}_{F\uparrow}) &= g^4 \int_{\ell, \ell_\tau} \left\{ \int_{q, q_\tau} [G_\downarrow(-\omega + q_\tau, -\mathbf{k}_{F\uparrow} + \mathbf{q})]^2 \right. \\ &\quad \left. D(q_\tau, \mathbf{q}) D(q_\tau + \ell_\tau, \mathbf{q} + \ell) \right\} \times \\ &\quad G_\uparrow(\omega + \ell_\tau, \mathbf{k}_{F\uparrow} + \ell) \\ &\equiv g^4 \int_{\ell, \ell_\tau} \left\{ C(\ell_\tau, \ell) \right\} G_\uparrow(\omega + \ell_\tau, \mathbf{k}_{F\uparrow} + \ell), \quad (11) \end{aligned}$$

where we will view the function $C(\ell_\tau, \ell)$ as a strongly frequency- and momentum dependent *intra-species* interaction. In local coordinate systems around the Fermi surfaces (cf. Fig. 8), the (on-shell) fermion propagator can be expressed as

$$G_\uparrow(\omega + \ell_\tau, \mathbf{k}_{F\uparrow} + \ell) = \frac{1}{-i(\omega + \ell_\tau) + v_{F\uparrow} \ell_\perp + \frac{1}{2m_\uparrow} (\ell_\perp^2 + \ell_\parallel^2)} \quad (12)$$

with Fermi velocity $v_{F\uparrow} = \sqrt{\frac{\mu_\uparrow}{2m_\uparrow}}$. The ℓ_\perp^2 term is subdominant in the infrared compared to the linear $v_{F\uparrow} \ell_\perp$ term. The Cooper

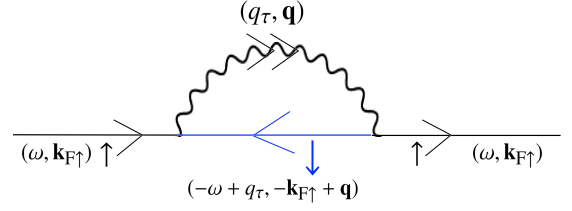


FIG. 10: (Color online) Infrared finite one-loop contribution to the fermion self-energy. The internal (blue) fermion line is always evaluated off-shell, that is, away from its Fermi surface. Note that in the different LOFF-case, where the Cooperon carries finite momentum, already this diagram can induce non-Fermi liquid behavior. This case is further discussed in Sec. II.

pair propagator at criticality is

$$D(q_\tau, \mathbf{q}) = \frac{1}{-iq_\tau + q_\tau^2 + \mathbf{q}^2} \quad (13)$$

where we may set the X - and Z -factors to unity here. Note that in an effectively particle-hole symmetric situations (in symmetric shells around the Fermi surfaces), the complex linear frequency term must vanish and the bare dynamical exponent would be $z = 1$. With disorder from trapping inhomogeneities or an additional species off which the Cooper pairs could scatter, one would have overdamped dynamics $\sim |q_\tau|$ [72].

Evaluating the *spin-down* fermions (the blue lines in the red box of Fig. 4) at the *spin-up* Fermi surface $\mathbf{k}_{F\uparrow}$ makes them off-shell and the infrared-dominant contribution of the dynamical intra-species interaction then comes from the two Cooper pair propagators

$$C_{\text{IR}}(\ell_\tau, \ell) \sim \int \frac{d^2 \mathbf{q}}{(2\pi)^2} \int \frac{dq_\tau}{2\pi} D(q_\tau, \mathbf{q}) D(q_\tau + \ell_\tau, \mathbf{q} + \ell) \quad (14)$$

which, for example, is logarithmically singular with a bare $z = 2$ power-counting. The precise form of the effective single-species interaction mediated by density fluctuations and two critical Cooperons also needs to account for the non-analyticities from pair-breaking effects from logarithm of the Cooperon, Eq. (C4), when summing over higher energy intermediate states as well as more precise experimental considerations such as trapping potentials and the presence of disorder. Upon closing this singular interaction with the on-shell spin-up fermion propagator Eq. (12) we conclude that the lifetime of quasiparticles cannot have the Fermi liquid form (where the interactions are regular and IR finite and $\text{Im}\Sigma_\uparrow(\omega, \mathbf{k}_{F\uparrow}) \sim \omega^2$) but instead will receive anomalous corrections.

A similar mechanism was shown to induce non-Fermi behavior in antiferromagnetic metals recently [54]. Strong non-Fermi liquid behavior (“hot Fermi surfaces”) and the total destruction of quasiparticles occurs for would require a strong-coupling re-summation of the logarithmic singularities of Eq. (14) as found by Abrahams *et al.* [49] in the spin-fermion model; such a re-summation would effectively lead to power-law, long-ranged interaction à la Bares and Wen [73].

Compared with the spin-density wave and Ising nematic quantum critical points in Table 2, the homogeneous imbalanced superfluid discussed in the present paper is expected to feature warm Fermi surfaces leading to anomalous thermodynamics and transport but, in the absence of band crossings/intersections of the two Fermi surfaces, ultimately stable quasi-particles. At the hot spots in the spin-density wave case ($\text{Im}\Sigma \sim \sqrt{\omega}$), or in the anti-nodal region of the nematic case ($\text{Im}\Sigma \sim \omega^{2/3}$), one has truly hot regions without any quasiparticles at all.

V. CONCLUSION AND OUTLOOK ON EXPERIMENTS

This paper has two main messages. First, we showed that quantum fluctuations may actually favor the appearance of exotic superfluids in two-dimensional, imbalanced mixtures of fermionic atoms. Second, our results put imbalanced fermionic superfluids on the map of plain vanilla quantum phase transitions (Fig. 2) in two spatial dimensions exhibiting non-Fermi liquid features. In light of the experimental progress in homogeneous trapping of fermionic atoms in reduced dimensionality, this paper hopefully stimulates that the results of mean-field approaches (applicable mostly to three-dimensional gases), will be carefully revisited in experiments and theory in two spatial dimensions.

Order parameter fluctuations, captured by solving a partial differential flow equation for the effective potential of the imbalanced Fermi gas, were shown to have dramatic beyond-mean-field effects on the zero-temperature phase diagram: for a range of parameters, a new, fluctuation-induced quantum critical point was found and Goldstone fluctuations were shown to destroy spontaneous symmetry breaking completely, in accordance with the Mermin-Wagner theorem.

We argued that this case is qualitatively different from the more frequently studied case of fermions coupled to gauge field and the hot spot phenomenology at the onset of antiferromagnetic order in metals. Its key features are:

(i) The collective mode(s) appears in the pairing channel spontaneously breaking the global $U(1)$ symmetry. This leads to a single Goldstone mode whose fluctuations were shown to turn the mean-field phase-separated ground state into a homogeneous, strongly coupled imbalanced superfluid with gapless fermion excitations. This also leads to different features in the quantum-critical field theory coupling two mismatched Fermi surfaces to the Cooperon. This bosonic Cooperon, for example, has a complex, linear time-derivative that leads to a non-trivial coupling of Goldstone and longitudinal couplings in the superfluid phase. It may additionally be Landau-damping from small disorder or trap inhomogeneities. Moreover, at the quantum critical point, one-loop vertex corrections renormalizing the Yukawa-coupling vanish by particle conservation - these structural novelties make a comprehensive, diagrammatic analysis of the coupled Fermi-Bose theory an interesting topic for future research.

(ii) Non-Fermi liquid physics around the Fermi surfaces appears although the Cooperon does not directly connect points or patches in the two mismatched Fermi surfaces. Repeated

scattering processes should lead to warm Fermi surfaces with reduced, non-Fermi liquid quasi-particle lifetimes.

(iii) The microscopic model of the parent compound is directly realizable in present-day experiments with ultra-cold mixtures of fermionic atoms. Techniques such as rf-spectroscopy [39, 46] bear the potential to measure the reduced fermion lifetimes. The frequency resolved rf-signal is proportional to the overlap of a non-interacting fermion propagator from a non-interacting third level with the interacting fermion and therefore should be able to resolve the single-particle self-energy [75]. Furthermore, one can measure the frequencies of collective Rabi oscillations directly which can be related to the quasi-particle weight, too [17].

The QCP's of Fig. 3 should also have observable consequences such as anomalous thermodynamics [6] up to relatively, high, finite temperatures in the quantum critical regime, even in a scenario in which it gets "masked" by p-wave superfluidity at the lowest scales. Finally, the collective modes such as sound and the longitudinal "Higgs" mode can also be measured for example by time-modulating the trapping potential and measuring the associated density response of the gas [74]. It would therefore be of great interest to generalize recent experiments with two-dimensional Fermi gases [76, 77] to Fermi mixtures [17] in the superfluid regime.

Acknowledgments

We acknowledge helpful discussions with Bertrand Delamotte, Nicolas Dupuis, Matthias Punk, Subir Sachdev, Brian Swingle, Tarik Yefsah, and Martin Zwierlein. The research of PS was supported by the DFG under grant Str 1176/1-1, by the NSF under Grant DMR-1103860, by the John Templeton Foundation, by the Center for Ultracold Atoms (CUA) and by the Multidisciplinary University Research Initiative (MURI). PJ acknowledges funding by the National Science Centre via 2011/03/B/ST3/02638.

Appendix A: Linking the flow to fermionic correlations

We here present the derivation of the mean-field effective potential Eq. (3) and the order parameter propagators Eq. (5) thereby providing a direct link of the order parameter flow to the underlying fermionic atoms.

We go to the thermodynamic limit and employ an action representation for Eq. (1). We perform a Hubbard-Stratonovich transformation with the spin-singlet pairing field ϕ_q conjugate to the fermion bilinear

$$\tilde{\phi}_q = g \int_k \psi_{k+\frac{q}{2}\uparrow} \psi_{-k+\frac{q}{2}\downarrow}. \quad (\text{A1})$$

We employ the short-hand notation $\int_k = T \sum_{k_0} \int \frac{d^2\mathbf{k}}{(2\pi)^2}$ with fermionic (imaginary) Matsubara frequencies $k_0 = 2\pi(n + 1/2)T$ with n integer running from $-\infty$ to ∞ . Their bosonic pendant is conventionally denoted by $q_0 = 2\pi nT$. Later we will take the zero temperature limit $T \rightarrow 0$ limit and focus

on ground state properties. The resulting functional integral is over ψ , $\bar{\psi}$ and ϕ with the new bare action

$$\begin{aligned} \mathcal{S}[\psi, \bar{\psi}, \phi] = & \int_k \sum_{\sigma=\uparrow, \downarrow} \bar{\psi}_{k\sigma}(-ik_0 + \xi_{\mathbf{k}\sigma}) \psi_{k\sigma} - \int_q \phi_q^* \frac{1}{g} \phi_q \\ & + \int_{k,q} \left(\bar{\psi}_{-k+\frac{q}{2}\downarrow} \bar{\psi}_{k+\frac{q}{2}\uparrow} \phi_q + \psi_{k+\frac{q}{2}\uparrow} \psi_{-k+\frac{q}{2}\downarrow} \phi_q^* \right), \end{aligned} \quad (\text{A2})$$

where ϕ^* is the complex conjugate of ϕ , while ψ and $\bar{\psi}$ are algebraically independent Grassmann variables. Note that as $g < 0$, the bosonic mass term $-1/g$ is positive.

We first shift ϕ_q by a non-fluctuating (static in time and homogenous in position space) field Δ :

$$\phi_q \rightarrow (2\pi)^2 \delta_{\mathbf{q},0} \frac{\delta_{\Omega,0}}{T} \Delta + \phi_q \quad (\text{A3})$$

where the factors of $(2\pi)^2$ are conventional and translate to the correct volume normalization factors in position space. Eq. (A2) is recast as $\mathcal{S} = \mathcal{S}_b + \mathcal{S}_f$ with

$$\mathcal{S}_b = \frac{(2\pi)^2}{T} |\Delta|^2 \left(\frac{-1}{g} \right) + \left(\frac{-1}{g} \right) (\Delta \phi_0^* + \Delta^* \phi_0) + \int_q \phi_q^* \phi_q \left(\frac{-1}{g} \right). \quad (\text{A4})$$

We employ a convenient Nambu matrix notation for the fermionic part

$$\begin{aligned} \mathcal{S}_f = & \int_k \overbrace{\left(\bar{\psi}_{k\uparrow} \ \psi_{-k\downarrow} \right)}^{\equiv \mathcal{S}_f^{(2)}[\Delta]} \begin{pmatrix} -ik_0 + \xi_{\mathbf{k}\uparrow} & -\Delta \\ -\Delta^* & -ik_0 - \xi_{-\mathbf{k}\downarrow} \end{pmatrix} \begin{pmatrix} \psi_{k\uparrow} \\ \bar{\psi}_{-k\uparrow} \end{pmatrix} \\ & + \int_{k,q} \left(\bar{\psi}_{k+\frac{q}{2}\uparrow} \ \psi_{-k+\frac{q}{2}\downarrow} \right) \begin{pmatrix} 0 & -\phi_q \\ -\phi_q^* & 0 \end{pmatrix} \begin{pmatrix} \psi_{k+\frac{q}{2}\uparrow} \\ \bar{\psi}_{-k+\frac{q}{2}\uparrow} \end{pmatrix}. \end{aligned} \quad (\text{A5})$$

This action is quadratic in the Grassmann fermion fields and we can perform the Gaussian functional integral. After expanding the resulting $\text{tr} \log$ to second order in ϕ_q , we obtain

$$\begin{aligned} \mathcal{S}[\phi] = & \int_q \phi_q^* \left(\frac{-1}{g} + K(q) \right) \phi_q + \int_q \phi_q^* \phi_{-q}^* \frac{L(q)}{2} + \int_q \phi_q \phi_{-q} \frac{L^*(q)}{2} \\ & - \frac{(2\pi)^2}{T} \frac{1}{g} |\Delta|^2 - \text{tr} \ln \beta \mathcal{S}_f^{(2)}[\Delta] \\ & + \left(\frac{-1}{g} \right) (\Delta \phi_0^* + \Delta^* \phi_0) - \left(\phi_0^* \int_k F_{f\uparrow\downarrow}(k) + \phi_0 \int_k F_{f\uparrow\downarrow}^*(k) \right), \end{aligned} \quad (\text{A6})$$

where the tr goes over Nambu indices, frequencies and momenta. The terms in the last line cancel, if Δ fulfills the saddle-point condition or gap equation

$$\Delta = -g \int_k F_{f\uparrow\downarrow}(k), \quad (\text{A7})$$

which is what one gets from differentiating the second line of Eq. (A6) with respect to Δ^* . Here, we have used the normal

(K) and anomalous (L) particle-particle pair propagators

$$\begin{aligned} K(q) &= - \int_k G_{f\uparrow}(k + \frac{q}{2}) G_{f\downarrow}(-k + \frac{q}{2}) \\ L(q) &= \int_k F_{f\uparrow\downarrow}(k + \frac{q}{2}) F_{f\downarrow\uparrow}(-k + \frac{q}{2}), \end{aligned} \quad (\text{A8})$$

and their single-particle constituents

$$\begin{aligned} G_{f\uparrow}(k) &= \frac{-ik_0 - \xi_{-\mathbf{k}\downarrow}}{(ik_0 - \xi_{\mathbf{k}\uparrow})(-ik_0 - \xi_{-\mathbf{k}\downarrow}) + |\Delta|^2} \\ F_{f\uparrow\downarrow}(k) &= \frac{\Delta}{(ik_0 - \xi_{\mathbf{k}\uparrow})(-ik_0 - \xi_{-\mathbf{k}\downarrow}) + |\Delta|^2}. \end{aligned} \quad (\text{A9})$$

To bring out the physics of Goldstone and longitudinal fluctuations, we now perform a change of variables in Eq. (A6), $\mathcal{S}[\phi] \rightarrow \mathcal{S}[\sigma, \pi]$, with

$$\begin{aligned} \phi_q &= \frac{\sigma_q + i\pi_q}{\sqrt{2}} \\ \phi_q^* &= \frac{\sigma_{-q} - i\pi_{-q}}{\sqrt{2}}, \end{aligned} \quad (\text{A10})$$

where π is the transversal Goldstone field variable and σ the radial Higgs field variable. Δ is chosen real and denoted by α such that

$$|\Delta|^2 = \frac{\alpha^2}{2} \equiv \rho. \quad (\text{A11})$$

The action obtains as

$$\begin{aligned} \mathcal{S}[\sigma, \pi, \alpha] = & \int_q \frac{\sigma_{-q} \sigma_q}{2} \left[-g^{-1} + K(q) + L(q) \right] \\ & + \int_q \frac{\pi_{-q} \pi_q}{2} \left[-g^{-1} + K(q) - L(q) \right] \\ & + \int_q \frac{\sigma_{-q} \pi_q}{2} \left(iK^{\text{odd}}(q) + i \frac{L^{*\text{odd}}(q) - L^{\text{odd}}(q)}{2} \right) \\ & + \frac{\pi_{-q} \sigma_q}{2} \left(-iK^{\text{odd}}(-q) + i \frac{L^{*\text{odd}}(-q) - L^{\text{odd}}(-q)}{2} \right) \\ & + \frac{(2\pi)^2}{T} U[\alpha], \end{aligned} \quad (\text{A12})$$

with $U[\alpha]$ the local effective potential given in Eq. (3) that survives $q \rightarrow 0$ mean-field limit. The mean-field phase diagram of Fig. 3 is determined by the field value α that globally minimizes the potential

$$\Omega^0(\mu, h, r, T) = \min_{\alpha} \{ U[\alpha] \}. \quad (\text{A13})$$

The $q \neq 0$ terms composed of fermionic pair propagators represent phase and amplitude fluctuations about the mean-field saddle-point. The superscript 'odd' projects out frequency and momentum components that transform odd under $q \rightarrow -q$. Because the anomalous pair propagator $L(q)$ of Eq. (A8) does not have an imaginary part, that is, $L^*(q) = L(q)$, the terms $\sim L$ in Eq. (A12) cancel.

The mass terms of the radial and Goldstone propagators can be obtained from derivatives of $U[\alpha]$. For the Goldstone propagator, one gets

$$\frac{1}{\alpha}U'[\alpha] \equiv \frac{1}{\alpha}\frac{\partial U}{\partial \alpha} = \frac{-1}{g} - \frac{1}{\alpha}\int_k F_{f\uparrow\downarrow}(k) = \frac{-1}{g} + K(0) - L(0), \quad (\text{A14})$$

where the second line uses the explicit expression of the pair propagators in Eq. (A8). The Goldstone mass is zero if $U'[\alpha_0] = 0$ or, equivalently, α_0 fulfills the saddle-point condition or gap equation. For the radial propagator, one gets

$$U''[\alpha] = \frac{\partial^2 U}{\partial \alpha^2} = \frac{1}{\alpha}\frac{\partial U}{\partial \alpha} + 2L(0) = \frac{-1}{g} + K(0) + L(0), \quad (\text{A15})$$

where we use Eq. (A14) to obtain the second line. $U''[\alpha_0]$ is finite providing the mass gap to the longitudinal fluctuations. We finally rewrite Eq. (A12) using Eqs. (A14,A15) to obtain:

$$\begin{aligned} S[\sigma, \pi, \alpha] &= \int_q \frac{\sigma_{-q}\sigma_q}{2} (Q_{\sigma\sigma}(q; \alpha) + U''[\alpha]) + \frac{(2\pi)^2}{T} U[\alpha] \\ &+ \int_q \frac{\pi_{-q}\pi_q}{2} \left(Q_{\pi\pi}(q; \alpha) + \frac{1}{\alpha}U'[\alpha] \right) \\ &+ \int_q \left(\frac{\sigma_{-q}\pi_q}{2} Q_{\sigma\pi}(q; \alpha) + \frac{\pi_{-q}\sigma_q}{2} Q_{\sigma\pi}(-q; \alpha) \right), \end{aligned} \quad (\text{A16})$$

with the momentum behavior of the propagators

$$\begin{aligned} Q_{\sigma\sigma}(q) &= K(q) + L(q) - (K(0) + L(0)) \\ Q_{\pi\pi}(q) &= K(q) - L(q) - (K(0) - L(0)) \\ Q_{\sigma\pi}(q) &= iK^{\text{odd}}(q). \end{aligned} \quad (\text{A17})$$

Clearly, $Q_{\sigma\sigma}(q=0) = Q_{\pi\pi}(q=0) = Q_{\sigma\pi}(q=0) = 0$.

Eqs. (A17) tie the renormalization group analysis for order parameter fluctuations Eq. (5) to the underlying fermionic correlations.

Appendix B: Details of the RG flow

We here give some details about the applied RG procedure. We restrict the momentum integrations to $|\mathbf{k}| < 3.5|\mathbf{k}_F| = 3.5 \times \sqrt{2}$ mimicking the UV-regularization of an attractive lattice Hubbard model at low filling fractions. In our computations, the initial momentum scale Λ_0 at which we start the flow is a free parameter. Generally, this should be momentum scale below which order parameter fluctuations are expected to kick in and we here take $\Lambda_0 = \sqrt{2} \sim |\mathbf{k}_F|$ attempting to account for an entire class of particle-hole and higher-order diagrams which are formally omitted within our truncation. These are expected to reduced ordering scales significantly [68].

The applied procedure is an adapted variant of a leading-order calculation in the functional renormalization-group derivative expansion. The next-to-leading order would also treat the Z - and X -factors as functions of ρ and Λ . Our main

focus here are the zero-temperature flows leading to the phase diagram in Fig. 3. For this situation a reliable approximation [78] neglects the order parameter flow of Z and X altogether and leaves their initial values at $\Lambda = \Lambda_0$ unchanged from the values guided by the form of the fermionic theory, Eqs. (A17), as well as attempting to account for particle-hole fluctuations and higher-order corrections. We here chose $Z_\Omega^{\Lambda_0} = Z_q^{\Lambda_0} = 1$, and $X^{\Lambda_0} = 0.2$.

Appendix C: Imbalanced particle-particle bubble

The imbalanced particle-particle bubble drawn in Fig. 9, whose low-energy expansion leads to the Cooper pair propagator Eqs. (9,13), is defined as

$$\Pi(q) = \Pi_{\text{pp}}(iq_\tau, \mathbf{q}) - \Pi_{\text{pp}}(0, 0), \quad (\text{C1})$$

with

$$\Pi_{\text{pp}}(iq_\tau, \mathbf{q}) = - \int_{-\infty}^{\infty} \frac{dk_\tau}{2\pi} \int_{-\infty}^{\infty} \frac{d^2\mathbf{k}}{(2\pi)^2} G_\uparrow(k+q/2)G_\downarrow(-k+q/2). \quad (\text{C2})$$

and

$$G_\sigma(k) = \frac{1}{-ik_\tau + \xi_{\mathbf{k}\sigma}} = \frac{1}{-ik_\tau + \frac{k^2}{2m_\sigma} - \mu_\sigma} \quad (\text{C3})$$

We can successively perform the integrations first k_τ , then k_x , and k_y last to find

$$\Pi(q) = \frac{-1}{4\pi} \log \left[1 + \frac{Q(q)}{2\mu} \right]. \quad (\text{C4})$$

where $\mu = \frac{1}{2}(\mu_\uparrow + \mu_\downarrow)$ and

$$Q(q) = Q(q_\tau, \mathbf{q}) = iq_\tau - \mathbf{q}^2 \left(\frac{1}{4m_r} - \frac{m_r}{16} \left(\frac{1}{m_\uparrow} - \frac{1}{m_\downarrow} \right)^2 \right). \quad (\text{C5})$$

The logarithm in Eq. (C4) will in general lead to branch cuts in the complex (frequency plane). For energies and momenta smaller than the effective binding energy 2μ , we can expand the logarithm to obtain Eq. (9) with

$$\begin{aligned} X &= \frac{1}{8\pi\mu} \\ Z_\Omega &= \frac{1}{32\pi\mu^2} \end{aligned} \quad (\text{C6})$$

$$Z_q = \frac{1}{32\pi\mu m_r} \left(1 - \frac{m_r^2}{4} \left(\frac{1}{m_\uparrow} - \frac{1}{m_\downarrow} \right)^2 \right), \quad (\text{C7})$$

where we further used the reduced mass $\frac{1}{m_r} = \frac{1}{2} \left(\frac{1}{m_\uparrow} + \frac{1}{m_\downarrow} \right)$.

- [1] L. D. Landau, *Theory of Fermi-liquids*, Sov. Phys. JETP **3**, 920 (1957); *Oscillations in a Fermi-liquid*, *ibid* **5**, 101 (1957).
- [2] P. Nozières, *Theory of Interacting Fermi Systems*, Benjamin, Amsterdam (1964).
- [3] A. J. Schofield, *Non-Fermi liquids*, Contemporary Physics **40**, 95 (1999).
- [4] C. M. Varma, Z. Nussinov, W. van Saarloos, *Singular or non-Fermi liquids*, Phys. Repts **361**, 267 (2002).
- [5] T. Schaefer, and K. Schwenzer, *Non-Fermi liquid effects in QCD at high density*, Phys. Rev. D **70**, 054007 (2004).
- [6] H. v. Löhneysen, A. Rosch, M. Vojta, and P. Woelfle, *Fermi-liquid instabilities at magnetic quantum phase transitions*, Rev. Mod. Phys. **79**, 1015 (2007).
- [7] P. Coleman, and A. J. Schofield, *Quantum criticality*, Nature **433**, 226 (2005).
- [8] S. Sachdev, and B. Keimer, *Quantum criticality*, Physics Today **64**, 29 (2011).
- [9] D. S. Greywall, *Specific heat of normal liquid ^3He* , Phys. Rev. B **27**, 2747 (1983).
- [10] D. Vollhardt, P. Woelfle, *The Superfluid Phases Of Helium 3*, Taylor & Francis (2003).
- [11] I. Bloch, J. Dalibard, and W. Zwerger, *Many-body physics with ultracold gases*, Rev. Mod. Phys. **80**, 885 (2008).
- [12] B. DeMarco, and D. S. Jin, *Onset of Fermi Degeneracy in a Trapped Atomic Gas*, Science **285**, 1703 (1999).
- [13] Z. Hadzibabic *et al.*, *Fiftyfold Improvement in the Number of Quantum Degenerate Fermionic Atoms*, Phys. Rev. Lett. **91**, 160401 (2003).
- [14] M. Koehl *et al.*, *Fermionic atoms in three dimensional optical lattice: Observing Fermi surfaces, dynamics, and interactions*, Phys. Rev. Lett. **94**, 80403 (2005).
- [15] M. Zwierlein *et al.*, *Fermionic Superfluidity with Imbalanced Spin Populations*, Science **311**, 492 (2006).
- [16] G. B. Partridge *et al.*, *Pairing and Phase Separation in a Polarized Fermi Gas*, Science **311**, 501 (2006).
- [17] C. Kohstall *et al.*, *Metastability and coherence of repulsive polarons in a strongly interacting Fermi mixture*, Nature **485**, 615 (2012).
- [18] W. V. Liu, and F. Wilczek, *Interior Gap Superfluidity*, Phys. Rev. Lett. **90**, 047002 (2003).
- [19] G. Sarma, *On the influence of a uniform exchange field acting on the spins of the conduction electrons in a superconductor*, J. Phys. Chem. Solids, **24**, 1029 (1963).
- [20] P. F. Bedaque, H. Caldas, and G. Rupak, *Phase Separation in Asymmetrical Fermion Superfluids*, Phys. Rev. Lett. **91**, 247002 (2003).
- [21] S.-T. Wu and S. Yip, *Superfluidity in the interior-gap states*, Phys. Rev. A **67**, 053603 (2003).
- [22] W. V. Liu, F. Wilczek, and P. Zoller, *Spin-dependent Hubbard model and a quantum phase transition in cold atoms*, Phys. Rev. A **70**, 033603 (2004).
- [23] A. Bulgac, M. McNeil Forbes, and A. Schwenk, *Induced P-Wave Superfluidity in Asymmetric Fermi Gases*, Phys. Rev. Lett. **97**, 020402 (2006).
- [24] M. M. Parish, F. M. Marchetti, A. Lamacraft, and B. D. Simons, *Polarized Fermi Condensates with Unequal Masses: Tuning the Tricritical Point*, Phys. Rev. Lett. **98**, 160402 (2007).
- [25] L. He, and P. Zhuang, *Phase diagram of a cold polarized Fermi gas in two dimensions*, Phys. Rev. A **78**, 033613 (2008).
- [26] S. Pilati, and S. Giorgini, *Phase Separation in a Polarized Fermi Gas at Zero Temperature*, Phys. Rev. Lett. **100**, 030401 (2008).
- [27] A. E. Feiguin, and M. P. A. Fisher, *Exotic Paired States with Anisotropic Spin-Dependent Fermi Surfaces*, Phys. Rev. Lett. **103**, 025303 (2009).
- [28] R. B. Diener, and M. Randeria, *BCS-BEC crossover with unequal-mass fermions*, Phys. Rev. A **81**, 033608 (2010).
- [29] L. Radzihovsky, and D. E. Sheehy, *Imbalanced Feshbach-resonant Fermi gases*, Rep. Prog. Phys. **73**, 076501 (2010).
- [30] A. Kujawa-Cichy and R. Micnas *Stability of superfluid phases in the 2D Spin-Polarized Attractive Hubbard Model* Europhys. Lett. **95**, 37003 (2011).
- [31] D. E. Sheehy, *Polarized superfluids near their tricritical point*, Phys. Rev. A **79**, 033606 (2009).
- [32] S. Yin, J.-P. Martikainen, and P. Torma, *Fulde-Ferrel states and Berezinskii-Kosterlitz-Thouless phase transition in two-dimensional imbalanced Fermi gases*, Phys. Rev. B **89**, 014507 (2014).
- [33] A. M. Clogston, *Upper limit for the critical field in hard superconductors*, Phys. Rev. Lett. **9**, 266 (1962).
- [34] K. Binder *Theory of first-order phase transitions*, Rep. Prog. Phys. **50**, 783 (1987).
- [35] H. v. Löhneysen, A. Rosch, M. Vojta, and P. Wölfle, *Fermi-liquid instabilities at magnetic quantum phase transitions*, Rev. Mod. Phys. **79**, 1015 (2007).
- [36] D. Belitz, T. R. Kirkpatrick, and T. Vojta, *How generic scale invariance influences quantum and classical phase transitions*, Rev. Mod. Phys. **77**, 579 (2005).
- [37] R. L. Greenblatt, M. Aizenman, and J.L. Lebowitz, *Rounding of First Order Transitions in Low-Dimensional Quantum Systems with Quenched Disorder*, Phys. Rev. Lett. **103**, 197201 (2009).
- [38] P. Jakubczyk, J. Bauer, and W. Metzner *Finite temperature crossovers near quantum tricritical points in metals*, Phys. Rev. B **82**, 045103 (2010).
- [39] J. T. Stewart, J. P. Gaebler, and D. S. Jin, *Using photoemission spectroscopy to probe a strongly interacting Fermi gas*, Nature **454**, 744 (2008).
- [40] Y. Liao *et al.*, *Spin-imbalance in a one-dimensional Fermi gas*, Nature **467**, 567 (2010).
- [41] A. J. A. James, and A. Lamacraft, *Non-Fermi-Liquid Fixed Point for an Imbalanced Gas of Fermions in $1+\epsilon$ Dimensions*, Phys. Rev. Lett. **104**, 190403 (2010).
- [42] D. E. Sheehy, and L. Radzihovsky, *BEC-BCS crossover, phase transitions and phase separation in polarized resonantly-paired superfluids*, Annals of Physics **322**, 1790 (2007).
- [43] R. M. Lutchyn, M. Dzero, and V. M. Yakovenko, *Spectroscopy of the soliton lattice formation in quasi-one-dimensional fermionic superfluids with population imbalance*, Phys. Rev. A **84**, 033609 (2011).
- [44] M. J. Wolak, B. Gremaud, R. T. Scalettar, and G. G. Batrouni, *Pairing in two-dimensional Fermi gas with population imbalance*, Phys. Rev. A **86**, 023630 (2012).
- [45] D. Roscher, J. Braun, and J. E. Drut, *Inhomogeneous phases in one-dimensional mass- and spin-imbalanced Fermi gases*, arXiv:1311.0179 (2013).
- [46] Z. Lan, G. M. Bruun, and C. Lobo, *Quasiparticle Lifetime in Ultracold Fermionic Mixtures with Density and Mass Imbalance*, Phys. Rev. Lett. **111**, 145301 (2013).
- [47] M. A. Metlitski, and S. Sachdev, *Quantum phase transitions of metals in two spatial dimensions: II. Spin density wave order*, Phys. Rev. B **82**, 075128 (2010).
- [48] J. Lee, P. Strack, and S. Sachdev, *Quantum criticality of re-*

- constructing Fermi surfaces in antiferromagnetic metals, *Phys. Rev. B* **87**, 045104 (2013).
- [49] E. Abrahams, J. Schmalian, and P. Woelfle, *Strong coupling theory of heavy fermion criticality*, arXiv:1303.3926.
- [50] V. Oganesyan, S. A. Kivelson, and E. Fradkin, *Quantum theory of nematic Fermi fluid*, *Phys. Rev. B* **64**, 195109 (2001).
- [51] W. Metzner, D. Rohe, and S. Andergassen, *Soft Fermi surfaces and Breakdown of Fermi-Liquid Behavior*, *Phys. Rev. Lett.* **91**, 066402 (2003).
- [52] S.-S. Lee, *Low-energy effective theory of Fermi surface coupled with $U(1)$ gauge field in 2+1 dimensions*, *Phys. Rev. B* **80**, 165102 (2009).
- [53] S. Powell, S. Sachdev, and H. P. Buechler, *Depletion of Bose-Einstein condensate in Bose-Fermi mixtures*, *Phys. Rev. B* **72**, 024534 (2005).
- [54] S. A. Hartnoll, D. M. Hofman, M. A. Metlitski, and S. Sachdev, *Quantum critical response at the onset of spin-density-wave order in two-dimensional metals*, *Phys. Rev. B* **84**, 125115 (2011).
- [55] P. Jakubczyk, W. Metzner, and H. Yamase, *Turning a First Order Quantum Phase Transition Continuous by Fluctuations: General Flow Equations and Application to d -Wave Pomeranchuk Instability*, *Phys. Rev. Lett.* **103**, 220602 (2009).
- [56] K. R. Patton, D. E. Sheehy, *Induced p -wave superfluidity in strongly interacting imbalanced Fermi gases*, *Phys. Rev. A* **83**, 051607 (R) (2011).
- [57] C. Langmack, M. Barth, W. Zwerger, and E. Braaten, *Clock Shift in a Strongly Interacting Two-Dimensional Fermi Gas*, *Phys. Rev. Lett.* **108**, 060402 (2012).
- [58] G. Bertainia, and S. Giorgini, *BCS-BEC Crossover in a Two-Dimensional Fermi Gas*, *Phys. Rev. Lett.* **106** 110403 (2011).
- [59] P. Bloom, *Two-dimensional Fermi gas*, *Phys. Rev. B* **12**, 125 (1975).
- [60] M. Randeria, J.-M. Duan, and L.-Y. Shieh, *Bound States, Cooper Pairing, and Bose Condensation in Two Dimensions*, *Phys. Rev. Lett.* **62**, 981 (1989).
- [61] A. J. Leggett, in *Modern Trends in the Theory of Condensed Matter*, edited by A. Pekalski and R. Przystawa (Springer, Berlin, 1980).
- [62] F. Pistolesi, C. Castellani, C. Di Castro, and G. C. Strinati, *Renormalization group approach to the infrared behavior of a zero-temperature Bose system*, *Phys. Rev. B* **69**, 024513 (2004).
- [63] P. Strack, R. Gersch, and W. Metzner, *Renormalization group flow for fermionic superfluids at zero temperature*, *Phys. Rev. B* **78**, 014522 (2008).
- [64] C. Wetterich, *Exact evolution equation for the effective potential*, *Phys. Lett. B* **301**, 90 (1993).
- [65] J. Berges, N. Tetradis, and C. Wetterich, *Non-perturbative renormalization flow in quantum field theory and statistical physics*, *Phys. Rep.* **363**, 223 (2002).
- [66] R. B. Diener, R. Sensarma, and M. Randeria, *Quantum fluctuations in the superfluid state of the BCS-BEC crossover*, *Phys. Rev. A* **77**, 023626 (2008).
- [67] B. Obert, C. Husemann, and W. Metzner, *Low-energy singularities in the ground state of fermionic superfluids*, *Phys. Rev. B* **88**, 144508 (2013).
- [68] L. P. Gorkov and T. K. Melik-Barkhudarov, *Contribution to the theory of superfluidity in an imperfect Fermi gas*, *Sov. Phys. JETP* **13**, 1018 (1961).
- [69] G. v. Gersdorff, and C. Wetterich, *Nonperturbative renormalization flow and essential scaling for the Kosterlitz-Thouless transition*, *Phys. Rev. B* **64**, 054513 (2001).
- [70] At finite temperatures the proposed truncation is not sufficient to describe the relevant BKT physics. Nevertheless, it is clear that also for $T > 0$ the flow at large Λ is dominated by the quantum terms and the initial evolution of the potential proceeds exactly along the same pattern. The additional thermal contributions are proportional to T and become relevant exclusively at large RG time (low Λ) where the structures of $U(\alpha)$ typical to a first-order transition had been smeared out by the flow. It is therefore a plausible scenario that a finite BKT transition line (drawn in Fig. 3) will connect the two newly found QCPs.
- [71] H. Yamase, P. Jakubczyk, and W. Metzner, *Nematic Quantum Criticality Without Order*, *Phys. Rev. B* **83**, 125121 (2011).
- [72] A. Del Maestro, B. Rosenow, and S. Sachdev, *Theory of pair-breaking superconductor-metal transition in nanowires*, *Annals of Physics* **324**, 523 (2009).
- [73] P.-A. Bares and X.-G. Wen, *Breakdown of the Fermi liquid due to long-range interactions*, *Phys. Rev. B* **48**, 8636 (1993).
- [74] E. Vogt *et al.*, *Scale-Invariance and Viscosity of a Two-Dimensional Fermi Gas*, *Phys. Rev. Lett.* **108**, 070404 (2012).
- [75] R. Haussmann, M. Punk, W. Zwerger, *Spectral functions and rf Response of Ultracold Fermionic Atoms*, *Phys. Rev. A* **80**, 063612 (2009).
- [76] M. Feld *et al.*, *Observation of a pairing pseudogap in a two-dimensional Fermi gas*, *Nature* **480**, 75 (2011).
- [77] B. Froehlich *et al.*, *Radio-Frequency Spectroscopy of a Strongly Interacting Two-Dimensional Fermi Gas*, *Phys. Rev. Lett.* **106**, 105301 (2011).
- [78] On the other hand, if taken into account, anomalous scaling of the propagator occurs exclusively at the transition and only once the fixed point is attained (at low Λ). Therefore our approximation should have no impact on our conclusions.